JOURNAL OF AGRICULTURAL AND FOOD CHEMISTRY

ARTICLE

pubs.acs.org/JAFC

Nanoemulsions of Cancer Chemopreventive Agent Benzyl Isothiocyanate Display Enhanced Solubility, Dissolution, and Permeability

Hussaini Syed Sha Qhattal,[†] Shu Wang,[#] Tri Salihima,[†] Sanjay K. Srivastava,[‡] and Xinli Liu*[,†]

[†]Department of Pharmaceutical Sciences and [‡]Department of Biomedical Sciences, School of Pharmacy, Texas Tech University Health Sciences Center, Amarillo, Texas 79106, United States

[#]Department of Nutrition, Texas Tech University, Lubbock, Texas 79409, United States

ABSTRACT: Benzyl isothiocyanate (BITC), a compound found in cruciferous vegetables, is an effective chemopreventive agent. The objective of this study was to develop nanoemulsion formulations for the oral delivery of BITC. Optimized oil-in-water BITC nanoemulsions were prepared by a spontaneous self-nanoemulsification method and a homogenization−sonication method. Both nanoemulsions entrapped high amounts of BITC (15−17 mg/mL), with low polydispersity and good colloidal stability. The BITC nanoemulsions showed enhanced solubility and dissolution compared to pure BITC. These formulations markedly increased the apical to basolateral transport of BITC in Caco-2 cell monolayers. The apparent permeability values were 3.6×10^{-6} cm/s for pure BITC and $(1.1-1.3) \times 10^{-5}$ cm/s for BITC nanoemulsions. The nanoemulsions were easily taken up by human cancer cells A549 and SKOV-3 and inhibited tumor growth in vitro. This work shows for the first time that BITC can be formulated into nanoemulsions and may show promise in enhancing absorption and bioavailability.

KEYWORDS: benzyl isothiocyanate, chemoprevention, nanoemulsion, self-nanoemulsifying drug delivery system, dissolution, Caco-2 permeability

INTRODUCTION

Chemoprevention through the use of dietary phytochemicals capable of delaying or preventing the carcinogenesis process is emerging as an important approach for cancer management. Oral consumption is the most desirable and acceptable form of delivery of chemopreventive agents as it provides flexibility of chronic dosing and is patient friendly. The effective oral delivery requires that the drugs have sufficient solubility in the gastrointestinal (GI) tract and good permeability to pass through the intestinal wall. However, the majority of chemopreventive agents are poorly water-soluble and, as such, cannot be solubilized in suitable pharmaceutical solvents with sufficient concentration or efficiently absorbed after oral administration.[1] Delivery of these agents via nanocarriers shows promise. For instance, curcumin, a dietary polyphenol chemopreventive agent, was formulated in poly(lactic-*co*-glycolic acid) (PLGA) microparticles and showed marked anticancer efficacy in breast cancer xenografts.[2] Additionally, epigallocatechin-3-gallate (EGCG), the major polyphenol from green tea, was encapsulated in submicrometer emulsions[3] or polysaccharide nanoparticles and showed efficacy against prostate cancer xenografts.[4]

Epidemiological studies indicate that a high dietary intake of cruciferous vegetables may reduce the incidence of human cancers.[5,6] Benzyl isothiocyanate (BITC, Figure 1), a sulfur-containing compound found in cruciferous vegetables such as garden cress,[7] has shown chemopreventive effects against chemical carcinogenesis in different types of preclinical cancer models, including lung, liver, intestinal, colon, breast, and pancreatic cancers.[8−11] The mechanism of BITC action was shown to be two-fold: inhibiting the phase I metabolism enzymes involved in the activation of carcinogens and induction of phase II detoxifying enzymes, responsible for elimination of carcinogens.[9,10] At the cellular level, BITC treatment has been shown to induce reactive oxygen species (ROS) formation, cause cell cycle arrest, induce apoptosis, and inhibit NFκB activation.[12−14] The bioavailability of BITC in human-consumed garden cress was found to be around 14−50%, as the active ingredient is not completely released from the vegetable by chewing.[7] Cooking of vegetables was shown to reduce the amount of available isothiocyanate by 2−6-fold compared to that available when the vegetables were consumed raw. In humans, about 54% of the administered BITC is metabolized to its *N*-acetylcysteine conjugate, which is excreted in urine.[15] Although BITC showed great promise in preclinical models, the translation to clinical investigation is hampered by a lack of suitable dosage form and poor bioavailability. We sought to develop formulations intended for oral delivery of the poorly water-soluble chemopreventive agent BITC.

Nanoemulsions are colloidal dispersions of nanosized oil droplets in an aqueous medium.[16,17] A recent review clarified that nanoemulsions (with size <300 nm) fundamentally differ from microemulsions with respect to stability (unlike microemulsions, nanoemulsions are thermodynamically unstable, but kinetically stable systems), preparation methods, and behavior toward dilution and temperature fluctuations.[18] Small droplet size and large surface area of dispersed phase give nanoemulsions high colloidal stability with fewer problems of inherent creaming, flocculation, coalescence, and sedimentation, which are commonly associated with conventional emulsions.[19] Nanoemulsions have

Received: June 30, 2011
Revised: October 18, 2011
Accepted: October 19, 2011
Published: October 19, 2011

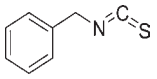

Figure 1. Structure of benzyl isothiocyanate (BITC).

been shown to improve in vitro dissolution and in vivo bioavailability of poorly water-soluble drugs.[20] Nanoemulsions can be prepared by high-energy dispersion techniques using mechanical devices to increase the water/oil interfacial area or by low-energy spontaneous emulsification methods such as a self-nanoemulsifying drug delivery system (SNEDDS), which is formed spontaneously by blending oil, water, surfactant, and cosurfactant, in the right proportion, with mild agitation. SNEDDS has emerged as a promising approach for the delivery of highly lipophilic drugs such as ritonavir (Norvir), cyclosporin A (Sandimmun Neoral), and saquinavir (Fortovase).[21]

Pure BITC is an oily liquid with poor aqueous solubility and high hydrophobicity (log P = 3); no formulation of BITC has been reported in the literature. We hypothesized that the oily nature of BITC could make it an ideal candidate to be formulated as an oil-in-water (o/w) nanoemulsion capable of facilitating administration and enhancing oral absorption. Our work shows for the first time that BITC nanoemulsions display enhanced solubility, dissolution, and permeability and may show promise in enhancing BITC absorption and bioavailability. The nanoemulsion formulation will potentially facilitate a chronic dosing regimen of BITC and support preclinical and clinical investigations of the cancer prevention efficacy of BITC.

MATERIALS AND METHODS

Chemicals. BITC (molecular weight 149), soybean oil, corn oil, olive oil, sulforhodamine B (SRB), and 1,2-benzenedithiol were purchased from Sigma-Aldrich (St. Louis, MO). Flaxseed oil was a gift from Jedwards International, Inc. (Quincy, MA). Medium-chain triglyceride oil was obtained from Nestle Nutrition (Ortho-Tek, Woodlands, TX). Tween 80 (polyoxyethylene sorbitan monooleate), Tween 20 (polyoxyethylene sorbitan monolaurate), glycerol, polyethylene glycol (PEG) 400, and methanol (HPLC grade) were purchased from Fisher Scientific (Pittsburgh, PA). Capryol 90 (propylene glycol monocaprylate) and Transcutol (diethylene glycol monoethyl ether) were obtained from Gattefosse (Toronto, ON, Canada). Egg L-α-phosphatidylcholine (PC, 95%) was purchased from Avanti Polar Lipids, Inc. (Alabaster, AL). 4,6-Diamidino-2-phenylindole (DAPI) was acquired from Invitrogen (Carlsbad, CA). All other chemicals used were purchased from Sigma-Aldrich and were of standard analytical grade or higher.

Cell Culture. Human colon cancer cells Caco-2, human ovarian cancer cells SKOV-3, and human epithelial lung carcinoma cells A549 were obtained from American Type Culture Collection (Manassas, VA). Caco-2 cells were cultured in EMEM supplemented with 20% fetal bovine serum (FBS; Gemini Bio-Products, Calabasas, CA). SKOV-3 cells were maintained in McCoy's 5A medium supplemented with 10% FBS and 10000 U/mL penicillin/streptomycin (Gibco, Invitrogen). A549 cells were maintained in RPMI-1640 medium (Irvine Scientific, Santa Ana, CA), supplemented with 10% FBS. Cells were grown in an incubator in an atmosphere of 5% CO_2 and 95% humidity.

BITC Solubility Study. The solubility of BITC in various oils (olive oil, flaxseed oil, corn oil, soybean oil, PEG-400, medium-chain triglycerides, Capryol 90) and distilled water was determined by adding 500 mg of BITC to 1 mL of the selected solvent and mixing with a shaker at 25 $\pm$ 2 °C for 24 h. The miscibility of BITC in different oils and water was checked by visual inspection. The samples were then centrifuged (Eppendorf Centrifuge 5415 C, Fisher Scientific) at 3000 rpm for 10 min in Ultrafree MC centrifugal filter units (MWCO 10000 Da, Millipore, MA). Undissolved BITC settled down into the filtrate compartment, and the supernatant with the BITC solubilized in oil was diluted 50000-fold in methanol; the concentration of BITC in the sample was quantified spectrophotometrically at 247 nm in a UV−visible spectrophotometer (GBC 918) on the basis of a BITC standard calibration curve with a linear range of 20−1500 μM. No oil interference was observed with the same dilution at this wavelength.

Nanoemulsion Preparation. Oil-in-water nanoemulsions were first prepared by a self-emulsification method. SNEDDS preformulation was carried out to identify suitable excipients with a potential to form nanoemulsions.[22] Briefly, surfactant mixtures (S_{mix}) were screened by using different weight ratios of primary surfactant (Tween 80 or Tween 20) and cosurfactant (Transcutol, propylene glycol, or ethanol) and studying the solubility of oils and BITC in these mixtures that yield a clear single-phase system. The optimal amount of surfactant mixture was determined as the maximal amount of S_{mix} that can solubilize the maximal amount of oil without forming a cloudy mixture. A pseudo-ternary phase diagram was constructed using a water titration method.[23] Surfactant was blended with cosurfactant at a fixed weight ratio (6:4) to obtain a surfactant mixture. Oil and the surfactant mixture (premix) were then mixed at weight ratios of 1:9, 2:8, 3:7, 4:6, 5:5, 6:4, 7:3, 8:2, and 9:1. The premix was titrated with water in a dropwise manner at room temperature under moderate agitation. The amount of aqueous phase added was varied to produce a water concentration in the range of 9−91% of the total volume. After equilibrium, the samples were visually checked and determined as being transparent gel, milky gel, milky emulsion, translucent nanoemulsion, or phase separation. Monophasic homogeneous systems were further characterized by appearance and droplet size. Transparent or translucent and easily flowable mixtures having a droplet size of <300 nm were designated nanoemulsions. Opaque milky dispersed systems were designated emulsions. For percentage transmittance analysis, formulations at a constant premix-to-water ratio of 1:10 were prepared by adding 1 g of premix dropwise to the 10 mL of water with agitation. The transmittance was measured against distilled water using a UV−visible spectrophotometer at 650 nm as reported.[24]

BITC nanoemulsions were also prepared by a homogenization−sonication technique using egg PC as an emulsifier.[25,26] Briefly, the aqueous phase was prepared using deionized water (4 mL) with 2.5% w/v glycerol and egg PC (0.5%). The oil phase, which comprised flaxseed oil (4.7%) with or without BITC (100 mg), was taken separately in a glass vial. The mass ratio of oil to egg PC was maintained at 10:1. Both oil and aqueous phases were heated at 70 °C for 2−3 min, followed by the gradual addition of the aqueous phase to the oil phase. This mixture was mixed rapidly using a magnetic stirrer and then homogenized at 6500 rpm for 2 min to form a coarse emulsion followed by homogenization at 9500 and 13500 rpm for 4 min using an Ultraturrax T25 homogenizer (IKA, Wilmington, NC) and bath sonication (Bransonic model 3510) for 120 min to yield the nanoemulsion. BITC encapsulation efficiency was analyzed by centrifuging 400 μL of the nanoemulsions in an Ultrafree-MC centrifugal filter (10000 MWCO, Millipore) at 11000 rpm for 30 min, and then supernatant was analyzed for BITC concentration. The entrapment efficiency was calculated as the percentage ratio between the amount of entrapped drug and the amount of total drug added. All nanoemulsions were stored at room temperature.

Droplet Size and Morphology Determination. Nanoemulsion droplet size and size distribution were analyzed using a dynamic light scattering technique on a particle sizing analyzer (Nicomp 380/ZLS, Santa Barbara, CA). The samples were diluted with deionized distilled water, and the average oil droplet diameter and the polydispersity index were determined. The morphology of nanoemulsions was determined by transmission electron microscopy (TEM). Briefly, a drop of sample was placed on a 200 square mesh copper grid and left to air-dry.

Negative staining consisted of 2% uranyl acetate for 2 min. After blotting and air-drying, images were obtained with a Hitachi H-7650 transmission electron microscope (Hitachi High-Technologies Corp., Pleasanton, CA).

Nanoemulsion Stability Analysis. The effect of pH of the aqueous phase on the droplet size and formation of nanoemulsions was evaluated by replacing deionized water with pH 1.2 simulated gastric fluid without pepsin (SGFsp), pH 4.7 (0.1 M sodium acetate) buffer, pH 6.8 (PBS) buffer, and pH 8.0 (0.1 M borate) buffer as aqueous phases. The effect of aqueous phase volume and subsequent dilution on droplet size of the formulations was analyzed by diluting the nanoemulsions 50-, 100-, and 1000-fold in aqueous phase with a 10 min lag time between dilution and particle size measurement. The stability of formulations was studied by centrifuging 1 mL of nanoemulsions at a speed of 3000 rpm for 25 min at room temperature.[27] The formulations were assessed for a change in droplet size, creaming, cracking, and phase separation.

In Vitro Dissolution Study. Dissolution studies of nanoemulsion formulations were performed according to the method described in USP 29/NF 24 using a USP rotating paddle dissolution apparatus II (Vankel VK 7900, Agilent Technologies, Santa Clara, CA) at 37 °C. Pure BITC oil or nanoemulsions with BITC equivalent to 100 mg were filled in empty gelatin capsules (size 00). The sinker was loaded with 900 mL of dissolution media (SGFsp, pH 1.2, USP 24) at 37 °C with a rotating speed of 50 rpm. Dialysis bags (MWCO 3500 Da) containing 10 mL of medium equilibrated for 12 h were used as the sampling ports as this yields true free drug concentration, avoiding the effects of unreleased drug from the nanoemulsions. One milliliter aliquots were removed from sampling ports at predetermined time intervals (10, 15, 30, 45, 60, 90, and 120 min) from the dialysis bags and replaced with 1 mL of fresh buffer. The amount of BITC released in the dissolution medium was determined spectrophotometrically.

Caco-2 Permeability Study. BITC transport from apical to basolateral compartment was measured in BD BioCoat fibrillar collagen 1.0 μm PET membrane 24-well cell culture inserts and intestinal epithelium differentiation environment following the manufacturer's instruction. About 200,000 Caco-2 cells were seeded per insert with a surface area of 0.3 cm^2. After differentiation, tight junctions were formed between Caco-2 cells. To evaluate the integrity of the Caco-2 monolayer, the transepithelial electrical resistance (TEER) across the monolayer was measured before and after drug transport using the Millicell Electrical Resistance System (Millipore Co., Bedford, MA). TEER reading for a monolayer of differentiated Caco-2 cells was between 300 and 500 ohms/cm^2. After the cell monolayer had been washed three times with PBS, cells were incubated at 37 °C with PBS, blank nanoemulsions, or 30 μM BITC pure drug and BITC nanoemulsions dissolved in 300 μL of PBS in the apical compartment. Aliquots of 500 μL of PBS were removed from the basolateral chamber (1 mL) at 0.5, 1, 2, 3, and 6 h. An equivalent volume of prewarmed PBS was added into the basolateral chamber after removal at each time. BITC concentration in the basolateral receiver compartment was measured by HPLC. The apical to basal apparent permeability (P_{app}, cm/s) was determined[28,29] according to the equation

$$P_{app} = \frac{dQ}{dt} \times \frac{1}{C_0} \times \frac{1}{A}$$

where dQ/dt is the rate of appearance of drug on the basolateral side, calculated from the cumulative amount versus time, C_0 is the initial concentration on the apical side, and A is the surface area of the membrane insert (0.3 cm^2).

Intracellular Delivery of Nanoemulsions. Fluorescent SRB dye was added in the oil phase and used as a probe to study the cellular uptake of nanoemulsions. SRB concentration was measured spectrophotometrically at 570 nm. A549 cells were plated at 0.5 million/well in a 6-well plate and allowed to attach overnight at 37 °C and 5% CO_2. Nanoemulsions were diluted in media to a final SRB concentration of 2 μM and were added to the cells for 2 h of incubation at 37 °C. Nucleus dye DAPI (2 μg/mL) was added 20 min before cells were imaged. After incubation, the medium was removed and the cells were washed with cold PBS three times; the uptake was studied under an Olympus IX 81 microscope. Images were captured with a Hamamatsu CCD camera using a constant exposure time (25 ms for blue channel and 100 ms for red channel). To quantify the intracellular uptake of BITC nanoemulsions, SKOV-3 cells were grown in a 100 mm Petri dish (2×10^6/dish). Pure BITC in ethanol or BITC nanoemulsions were added to cells at the final BITC concentration of 10 μM and incubated at 37 °C for 3 h. Cells were washed with PBS and lysed, and the intracellular concentration of the BITC was analyzed by HPLC. The protein concentrations were determined using the bicinchoninic acid (BCA) assay.

HPLC Analysis of BITC. BITC concentrations from the Caco-2 permeability study and uptake assays were analyzed on the basis of a published HPLC method.[30] Briefly, BITC-containing samples were derivatized with 1,2-benzenedithiol to produce 1,3-bezenedithiol-2-thione, which was extracted with hexane and had an absorption at 365 nm. HPLC analysis was carried out in a Waters 2695 separation module equipped with a 2489 UV−vis detector and a reversed-phase liquid chromatography (4.6 × 150 mm) C18 column. The mobile phase consisted of methanol and water (85:15, v/v) at a flow rate of 0.7 mL/min. 1,3-Benzenedithiol-2-thione had a retention time of 5.6 min.

Cytotoxicity Analysis. All cytotoxicity assays were performed in 96-well plates using a SRB colorimetric assay.[31] Cells were plated at 1000−2500 cells/well in 100 μL of complete medium. After overnight incubation to allow attachment, pure BITC in ethanol or nanoemulsions were diluted to final concentrations of 5, 10, 15, or 20 μM in 100 μL of medium in replicates of 16 wells per condition. Control wells received ethanol or blank emulsions in complete medium equivalent to the maximum final ethanol concentration of drug-treated wells. After a 96 h incubation period, cell monolayers were fixed with 10% (w/v) trichloroacetic acid and stained with SRB solution for 30 min, after which excess dye was removed by repeated washings with 1% (v/v) acetic acid. The protein-bound dye was dissolved in 10 mM Tris base solution for optical density determination at 570 nm using a microplate reader (BioTek Instruments, Inc., Winooski, VT).

Statistical Analyses. All of the values are reported as the mean ± standard deviation (SD). All statistical analyses were done using GraphPad Prism 5 software (San Diego, CA). Differences between two means were tested using an unpaired, two-sided Student's t test. Cytotoxicity curve comparison was performed by two-way ANOVA followed by Bonferroni's post-test analysis. Differences with $p < 0.05$ were considered to be significant.

RESULTS AND DISCUSSION

Preparation and Optimization of BITC Nanoemulsions. The oily nature of BITC prompted us to formulate it as a nanoemulsion. High solubility of drug in the oil phase is an important criterion for making nanoemulsions, as it determines the nanoemulsion's ability to maintain the drug in solubilized form. Figure 2 shows that BITC was completely miscible in all seven oils screened, with solubility values ranging from 170 to 270 mg/mL. In contrast, BITC is poorly water-soluble, with an aqueous solubility of 0.16 ± 0.03 mg/mL (Figure 2). We selected medium-chain triglycerides (MCT) and flaxseed oils as primary oil phases for nanoemulsion preparation for the following reasons. MCT has many advantages in the formulation of nanoemulsions ranging from their regulatory status (approved for pharmaceutical injection) to their absorption enhancement of formulated drugs.[32−34] MCT is suitable for encapsulating drugs with log P value ranging from 2 to 4.[35]

We chose flaxseed oil mainly on the basis of its chemoprevention effects. Flaxseed oil rich in polyunsaturated ω-3 fatty acid (mainly α-linolenic acid) has been used in formulating drugs to enhance bioavailability. The consumption of flaxseed oil can suppress pro-inflammatory cytokines, including tumor necrosis factor-α (TNF-α) and interleukin-1-β (IL-1β), which have been linked to increased colon cancer risk.[36] Dietary flaxseed oil is effective in preventing colon tumor development when compared with dietary corn oil containing ω-6 fatty acids in rats.[37−39]

First, we formulated nanoemulsions by self-emulsification methods in which MCT was used as the oil phase. Excipients screening and formulation optimization of nanoemulsions were based on the following criteria: (1) the formation of nanoemulsions should be simple and fast; (2) droplet size should be smaller than 300 nm, and no phase separation should be visible after storage for 24 h; and (3) it should be able to achieve high drug loading, small and uniform droplet size (small polydispersity index), and rapid dispersion upon dilution with an aqueous medium.[40] The right blend of surfactants with high and low hydrophilic lipophilic balance (HLB) value is important in forming the stable o/w nanoemulsion formulations.[41] We selected nonionic surfactant Tween 80 (HLB = 15) as primary surfactant because it is less toxic than ionic surfactant and well miscible with BITC. Transcutol (HLB = 4.2) was selected among ethanol (HLB = 7.9) and propylene glycol (HLB = 11.6) as a cosurfactant to support the generation of stable interfacial film.[42]

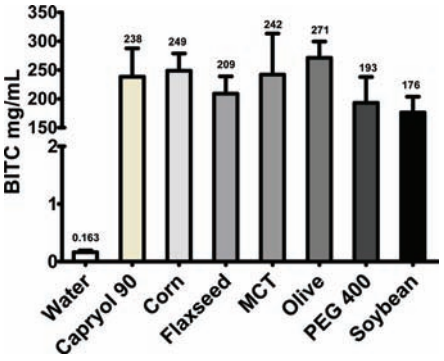

Figure 2. Solubility of BITC in water and different oils.

Transcutol is nonionic, miscible with BITC oil, and known to increase the permeability of drugs.[43] Preformulation showed that Tween 80 and Transcutol at a weight ratio of 6:4 produced high BITC and oil solubility and ease of redispersibility. Together, the surfactant mixtures provide a blend of both high and low HLB surfactants to make stable nanoemulsions.

The phase diagram of the pseudoternary system of MCT oil/S_{mix} (Tween 80:Transcutol = 6:4)/water is shown in Figure 3A. Areas of the phase diagram containing single-phase translucent nanoemulsion, opaque milky emulsion, transparent gel, and milky gel regions were identified. Formulations at a constant premix-to-water ratio of 1:10 (w/w) were chosen for further investigation (Table 1). The mean droplet sizes were largely dependent on the ratio of the oil-to-surfactant mixture (oil/S_{mix}, w/w). When the ratios were lower than 0.67, the mean droplet sizes of the nanoemulsions formed spontaneously were <300 nm (Table 1; Figure 3B). When the oil/S_{mix} ratio ranged from 9.0 to 2.3, phase separation was seen. Between these ratios, the droplet sizes of the emulsions were close to or greater than 500 nm. Measuring optical transmittance (Table 1) provides an indication of formation of translucent or transparent nanoemulsions, as the small droplet sizes lead to increased percentage transmittance.[44] When the oil/S_{mix} ratio was <0.67 (SN-8, SN-9, SN-10, and SN-11 formulations, Figure 3B), translucent dispersion was observed (% transmittance was 30−100%); when the ratio was between 1.0 and 1.5 (SN-6 and SN-7), milky or cloudy preparation was observed; and finally, when the ratio was >2 (SN-3, SN-4, and SN-5), phase separation was observed. On the basis of the phase diagram, droplet size, and percentage transmittance results, the transparent and stable nanoemulsion SN-10 was selected as an optimized SNEDDS for further evaluations (Table 2). SN-10 contains the minimum concentration of S_{mix} and a high percentage of aqueous phase to avoid irritation and precipitation of the drug on dilution in the gut lumen in vivo. When the oily BITC was incorporated into the SN-10 formulation, no change in phase behavior of the system was evident.

High-energy emulsification techniques such as microfluidization and ultrasonication have been frequently used to produce nanoemulsions.[25,26,45] Next, we prepared nanoemulsions using a homogenization−sonication method. The optimized FLNE-4 formulation consisted of flaxseed oil as the oil phase and egg PC

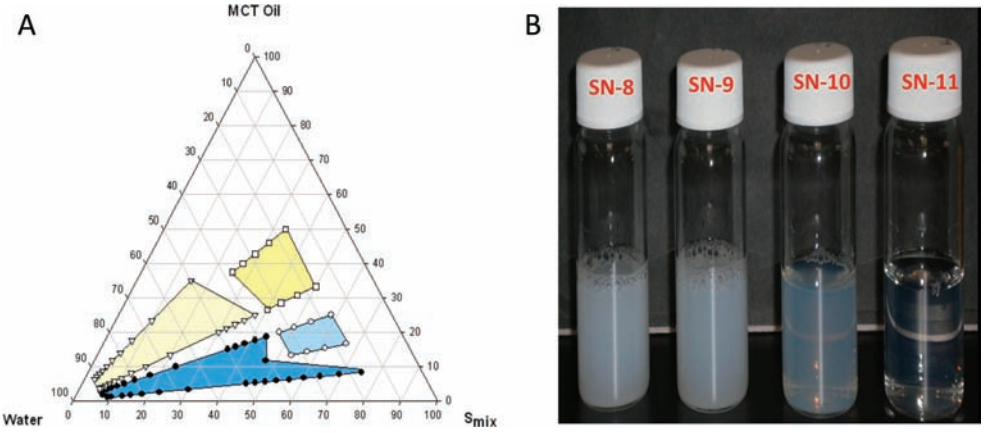

Figure 3. (A) Pseudoternary phase diagram of MCT (oil), Tween 80/transcutol (S_{mix}, ratio 6:4), and water system. The formulations tested are marked in the phase diagram. The solid circles (●) represent the translucent nanoemulsions, the open squares (□) represent milky gels, the open circles (○) represent transparent gels, and the open triangles (△) represent the opaque milky emulsions. (B) Photographs of SNEDDS formulations with droplet size below 300 nm.

Table 1. Formulation Composition, Percent Transmittance, and Droplet Size of Self-Emulsified Formulations[a]

formulation code	oil	surfactant	cosurfactant	surfactant: cosurfactant	ratio (oil:S_{mix})	% transmittance	particle size (nm)	PI
SN-3	MCT	Tween 80	Transcutol	6:4	9:1 (9.0)	53.1	PS	
SN-4	MCT	Tween 80	Transcutol	6:4	8:2 (4.0)	21.4	PS	
SN-5	MCT	Tween 80	Transcutol	6:4	7:3 (2.33)	37.2	PS	
SN-6	MCT	Tween 80	Transcutol	6:4	6:4 (1.5)	22.8	>500	
SN-7	MCT	Tween 80	Transcutol	6:4	5:5 (1.0)	14.0	476 ± 116	0.464
SN-8	MCT	Tween 80	Transcutol	6:4	4:6 (0.67)	30.3	221 ± 40	0.399
SN-9	MCT	Tween 80	Transcutol	6:4	3:7 (0.43)	53.6	179 ± 39	0.153
SN-10	MCT	Tween 80	Transcutol	6:4	2:8 (0.25)	94.3	107 ± 23	0.212
SN-11	MCT	Tween 80	Transcutol	6:4	1:9 (0.11)	99.2	35.8 ± 11	0.272

[a] S_{mix} refers to weight ratios of surfactant and cosurfactant. Samples were made at a constant premix (mixture of oil and S_{mix})-to-water ratio of 1:10 (w/w). PI value refers to polydispersity index and PS refers to phase separation.

Table 2. Formulation Composition and BITC Entrapment Efficiency of Optimized Nanoemulsions Prepared by Homogenization−Sonication Method (FLNE-4) and Self-Emulsification Method (SN-10)

formulation	oil (O)	surfactant (S)	ratio O:S	BITC (mg/mL)	volume of water (%)	entrapment efficiency (%)	droplet size (nm)	PI
FLNE-4	flax seed	egg PC	10:1	17	95	77	242 ± 3	0.141
SN-10	MCT	Tween 80: Transcutol (6:4)	2:8	15	91	70	117 ± 27	0.185

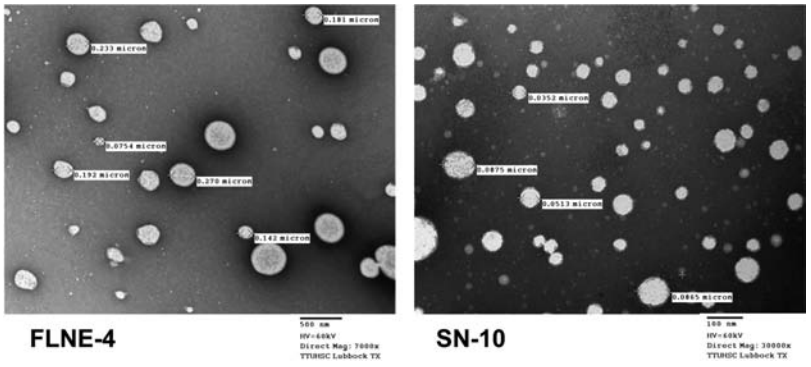

Figure 4. TEM images of the optimized nanoemulsions.

served as a nontoxic emulsifier, and its composition is presented in Table 2.

Particle Size, Morphology, and BITC Encapsulation Efficiency. Physical characteristics of the two lead nanoemulsions prepared by the above two methods are listed in Table 2. FLNE-4 formulation prepared by homogenization−sonication method had bigger droplet size (242 ± 3 nm) than the SN-10 (117 ± 27 nm) formulation that was prepared via self-emulsification method. This is consistent with the literature that high-energy methods normally do not yield oil droplet radii of <100 nm unless an extremely high disruptive force is applied.[46] BITC is most effective in the 7−30 μM concentration range. Considering the relatively high effective concentration and the in vivo metabolic instability and short half-life of BITC,[10] an oral dosage form of BITC should have high drug loading and stability. Both nanoemulsions entrapped high amounts of BITC (15−17 mg/mL) with high efficiency (>70%) (Table 2), exceeding the maximal amount of BITC (0.16 mg/mL) that can be dissolved in water. The formulations had minimal size distribution, as demonstrated by polydispersity indices of <0.2 (Table 2). TEM images (Figure 4) showed that both formulations had spherical droplets, with sizes that were slightly smaller than those measured by the dynamic light scattering technique (Table 2). The slightly lower droplet sizes of the formulations from the TEM images compared to the droplet sizes obtained from the dynamic light scattering measurements are in good agreement with the literature.[47]

Nanoemulsion Stability. Formulation SN-10 demonstrated good stability in acidic environment (SGFsp, pH 1.2) and no significant changes in the droplet size over the entire range of pH (1.2−8.0) tested (Figure 5A). Compared with distilled water, the particle size of FLNE-4 formulation increased significantly in pH 1.2 SGFsp solution, but remained stable at pH 4.7−8.0 (Figure 5B). Dilutions up to 1000-fold in water had no significant effects on the droplet sizes of both nanoemulsions, and no phase separation was observed (Figure 5C). Additionally, centrifugal stress had minimal effect on the mean droplet sizes of nanoemulsions (Figure 5D). The nanoemulsions are stable at room temperature for at least 3 months without any substantial changes of droplet sizes and physical appearance.

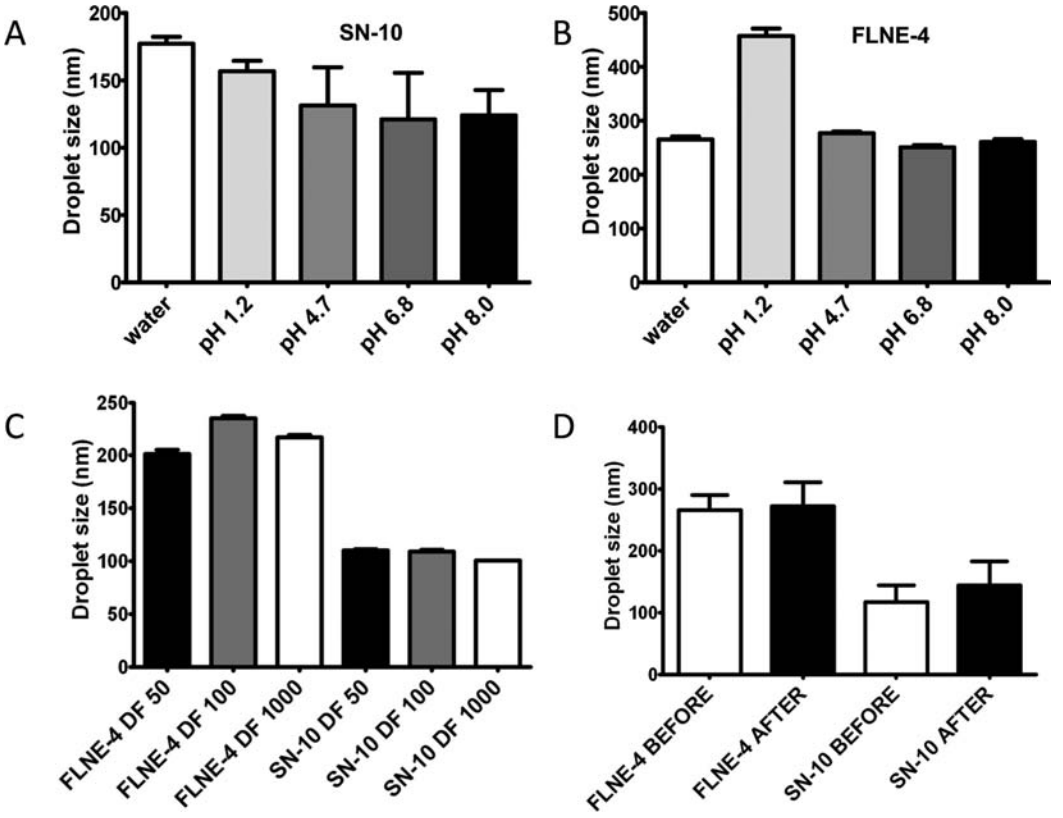

Figure 5. Effects of aqueous phase pH (A, B), dilution (C), and centrifugal stress (D) on droplet size of SN-10 and FLNE-4 nanoemulsions. DF refers to dilution factor.

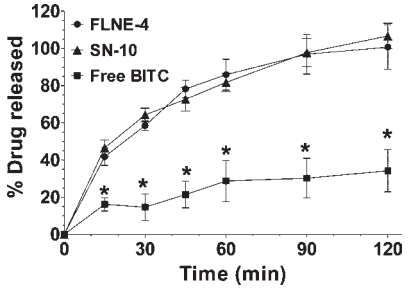

Figure 6. Dissolution studies of pure BITC and BITC nanoemulsions in dissolution media (SGFsp, pH 1.2). Data are presented as the mean ± SD, $n = 3$; ∗ represents $p < 0.001$ after two-way ANOVA, followed by Bonferroni's multiple-comparison test.

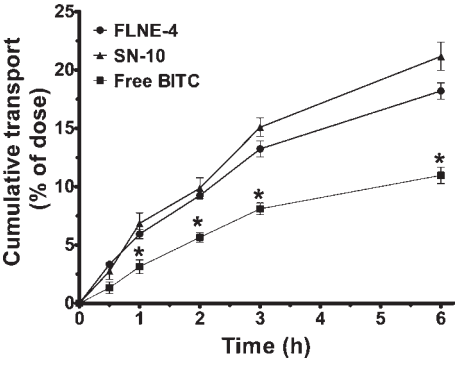

Figure 7. Time course of pure BITC and BITC nanoemulsion transport across Caco-2 monolayers. Data are presented as the mean ± SD, $n = 3$; ∗ represents $p < 0.001$ after two-way ANOVA, followed by Bonferroni's multiple-comparison test.

BITC Nanoemulsion Dissolution Study. We compared the dissolution behavior of BITC-loaded SN-10 or FLNE-4 nanoemulsions with that of the pure BITC in simulated gastric fluid. As shown in Figure 6, dissolution of pure BITC was poor in SGFsp (pH 1.2), with only 34% of the drug going into the dissolution medium at the end of the 2 h run. The poor dissolution of BITC can be attributed to its hydrophobic nature and poor wettability. Both SN-10 and FLNE-4 nanoemulsions displayed significantly faster dissolution rates than pure BITC in acidic simulated gastric fluid. Up to 80% of the drug was released within 60 min; nearly 100% of the drug was released by the end of the 2 h dissolution test. Dissolution of BITC from both nanoemulsions was significantly higher ($p < 0.001$) than that from the pure BITC at every time point measured, likely because the nanoemulsions enhance the drug solubility and promote effective dispersion of hydrophobic drug in the dissolution media. SN-10 and FLNE-4 nanoemulsions showed no significant difference in their dissolution rates (Figure 6). For poorly water-soluble drugs, the absorption rate from the GI tract is controlled by the rate and extent of dissolution of drug from dosage forms.[48] The results suggest that nanoemulsions are promising nanocarriers that may enhance the oral absorption of BITC.

Drug Transport in the Caco-2 Monolayer. The nanosized droplets with increased interfacial area can also influence the transport properties of drugs.[49] Caco-2 cell monolayer can be used as a model membrane of the intestinal epithelium. It was

demonstrated that the amount of drug that permeates to the basal side of the Caco-2 monolayers correlates to drug permeability across the human intestine [28,50,51] and drug absorption in humans.[52−56] Treatment with the pure BITC or BITC nanoemulsions showed no significant change in TEER compared with the PBS or blank nanoemulsions treated controls throughout the experiments, which confirms the tight junction integrity of the differentiated Caco-2 monolayers. As shown in Figure 7, the cumulative amount of BITC transported across Caco-2 monolayers in the absorptive (apical to basolateral) direction increased significantly in SN-10 and FLNE-4 nanoemulsions as compared to the pure BITC. The apparent permeability values (P_{app}) were calculated from the slopes of the Caco-2 transport profile and summarized in Table 3. Both nanoemulsions demonstrated significantly higher ($p < 0.001$) rate and extent of absorption than the pure BITC. The apparent permeability P_{app} of BITC free drug was 3.6×10^{-6} cm/s. Previous studies reported compounds with P_{app} values of $(1-10) \times 10^{-6}$ cm/s as being moderately absorbed molecules.[48] The nanoemulsion carriers improved P_{app} for BITC by nearly 3-fold. This could be due to the increased surface areas of droplets leading to improved surface contact with biological membrane and the influences of formulation excipients on membrane fluidity and permeability. There was no significant difference in apparent permeability between SN-10 and FLNE-4 nanoemulsions (Table 3). The results suggest that nanoemulsions may enhance the transport of BITC in the intestinal epithelium.

Table 3. P_{app} Values of BITC and Its Nanoemulsions Determined by Caco-2 Assays

category	average apparent permeability, P_{app} (cm/s)
free BITC	3.6×10^{-6}
SN-10	1.3×10^{-5}
FLNE-4	1.1×10^{-5}

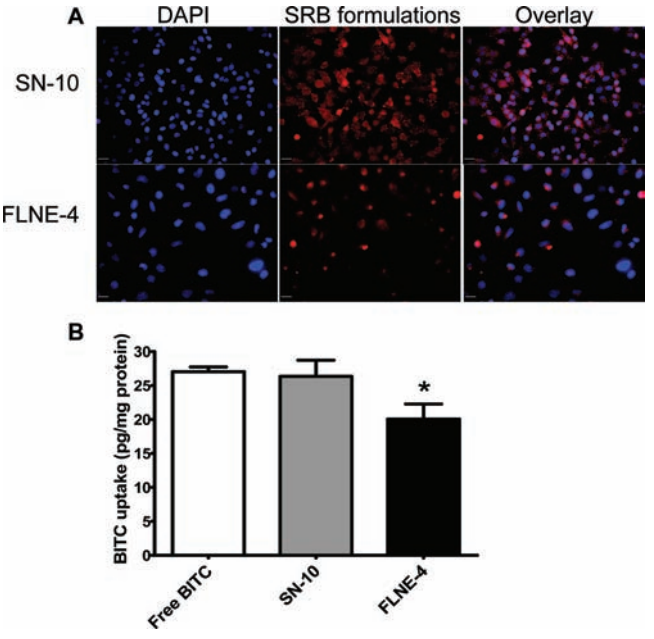

Figure 8. (A) Fluorescence images of cellular uptake of SRB loaded nanoemulsions after 2 h of exposure in A549 cells. Cell nuclei were stained blue by DAPI, and nanoemulsions display red fluorescence. The overlay images show the cellular association of the nanoemulsions. (B) HPLC analysis of intracellular accumulations of BITC delivered as pure drug in ethanol or in nanoemulsions after 2 h of exposure in SKOV-3 cells. The bars represent the mean ± SD of each treatment, $n = 3$; ∗ represents $p < 0.01$ after Student's t test.

Cellular Uptake and Intracellular Delivery of Nanoemulsions. Cellular uptake of nanoemulsions was studied by fluorescence microscopy using fluorescent dye SRB loaded formulations. Both nanoemulsions were taken up into cells, evidenced by the red fluorescence (SRB nanoemulsions) around blue nuclei (DAPI) (Figure 8A). SN-10 formulation showed higher uptake compared to FLNE-4 within 2 h of treatment (Figure 8A). The intracellular delivery of nanoemulsions was further quantified using the HPLC method after 2 h of exposure of SKOV-3 cells to pure BITC in ethanol or nanoemulsions (Figure 8B). The total amount of BITC delivered intracellularly by the SN-10 formulation (26.3 ± 2.4 pg/mg protein) was equivalent to that by the pure drug in ethanol vehicle (27.1 ± 0.7 pg/mg protein). Consistent with the fluorescence uptake study, FLNE-4 delivered significantly lower BITC (20.1 ± 2.2 pg/mg protein, $p < 0.05$) intracellularly compared to the pure BITC and SN-10 (Figure 8). This could be attributed to the higher mean droplet size of the FLNE-4 formulation compared to the SN-10 formulation (Table 2).

Growth Inhibitory Effects of BITC Nanoemulsion. To study the intracellular release of BITC from nanoemulsions, cytotoxicity analyses were performed in human lung cancer A549 and ovarian cancer SKOV-3 cells (Figure 9). Blank nanoemulsion vehicles were not toxic to the cells at the concentrations used in the study (data not shown). SN-10 nanoemulsion achieved equivalent cytotoxicity as compared to the free drug, but FLNE-4 kills statistically fewer cells over 4 days of incubation ($p < 0.05$) (Figure 9). The data suggest that BITC is released from nanoemulsion droplets, causing cytotoxicity. Even though the SN-10 and FLNE-4 nanoemulsions did not show any significant differences in their dissolution and permeability, SN-10

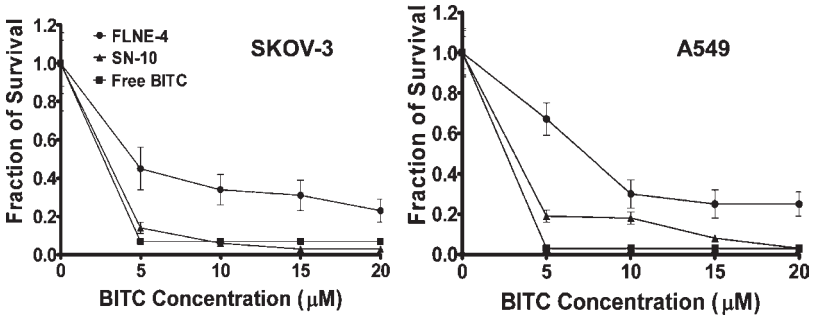

Figure 9. Cytotoxicity of pure BITC in ethanol or in nanoemulsions in SKOV-3 and A549 cells analyzed by the SRB assay.

nanoemulsion displayed higher intracellular BITC delivery and increased cytotoxicity in comparison to the FLNE-4 formulation. This is likely related to the smaller size of SN-10 formulation, as previous papers have shown an increase in lipid digestion rate with decreasing droplet size.[57,58] The lower cytotoxicity observed with FLNE-4 could be attributed to the lower drug uptake into the cancer cells as seen in the uptake studies (Figure 8). Higher uptakes and increased cytotoxicity of the pure drug were due to the ethanolic vehicle, which provides unhindered passage of free drug through the cell membranes. On the basis of the advantages of SNEDDS formulation, the SN-10 oral nanoemulsion was selected for further in vivo pharmacokinetics and chemoprevention efficacy evaluations.

In conclusion, we encapsulated a promising chemopreventive agent, BITC, into nanoemulsions. Optimized o/w nanoemulsion SN-10 was prepared by the SNEDDS method, and FLNE-4 nanoemulsion was prepared by the homogenization−sonication method. Both nanoemulsions entrapped high amounts of BITC (15−17 mg/mL), with low polydispersity and good colloidal stability. The formulations displayed fast dissolution and high permeability, efficiently released the drug intracellularly, and inhibited cancer cell growth in vitro. Our work shows for the first time that nanoemulsions are promising nanocarriers that may increase the absorption and bioavailability of BITC.

AUTHOR INFORMATION

Corresponding Author

*Postal address: Department of Pharmaceutical Sciences, School of Pharmacy, Texas Tech University Health Sciences Center, 1406 Coulter Drive, Suite 1105, Amarillo, TX 79106. Phone: (806) 356-4750, ext 226. Fax: (806) 356-4770. E-mail: xinli.liu@ttuhsc.edu.

Funding Sources

This work was funded by the Texas Tech University Health Sciences Center (TTUHSC) School of Pharmacy (X.L.).

ACKNOWLEDGMENT

Electron microscopy was performed by Charles Linch at the Medical Photography and Electron Microscopy Center at TTUHSC. We thank Dr. Reza Mehvar from TTUHSC for critically reading the manuscript.

REFERENCES

(1) Weingart, S. N.; Brown, E.; Bach, P. B.; Eng, K.; Johnson, S. A.; Kuzel, T. M.; Langbaum, T. S.; Leedy, R. D.; Muller, R. J.; Newcomer, L. N.; O'Brien, S.; Reinke, D.; Rubino, M.; Saltz, L.; Walters, R. S. NCCN Task Force Report: Oral Chemotherapy. *J. Natl. Compr. Cancer Netw.* **2008**, *6* (Suppl. 3), S1–S14.

(2) Shahani, K.; Swaminathan, S. K.; Freeman, D.; Blum, A.; Ma, L.; Panyam, J. Injectable sustained release microparticles of curcumin: a new concept for cancer chemoprevention. *Cancer Res.* **2010**, *70* (11), 4443–4452.

(3) Ru, Q.; Yu, H.; Huang, Q. Encapsulation of epigallocatechin-3-gallate (EGCG) using oil-in-water (O/W) submicrometer emulsions stabilized by iota-carrageenan and beta-lactoglobulin. *J. Agric. Food Chem.* **2010**, *58* (19), 10373–10381.

(4) Rocha, S.; Generalov, R.; Pereira Mdo, C.; Peres, I.; Juzenas, P.; Coelho, M. A. Epigallocatechin gallate-loaded polysaccharide nanoparticles for prostate cancer chemoprevention. *Nanomedicine (London)* **2011**, *6* (1), 79–87.

(5) Le Marchand, L.; Yoshizawa, C. N.; Kolonel, L. N.; Hankin, J. H.; Goodman, M. T. Vegetable consumption and lung cancer risk: a population-based case-control study in Hawaii. *J. Natl. Cancer Inst.* **1989**, *81* (15), 1158–1164.

(6) Verhoeven, D. T.; Goldbohm, R. A.; van Poppel, G.; Verhagen, H.; van den Brandt, P. A. Epidemiological studies on brassica vegetables and cancer risk. *Cancer Epidemiol. Biomarkers Prev.* **1996**, *5* (9), 733–748.

(7) Vermeulen, M.; van den Berg, R.; Freidig, A. P.; van Bladeren, P. J.; Vaes, W. H. Association between consumption of cruciferous vegetables and condiments and excretion in urine of isothiocyanate mercapturic acids. *J. Agric. Food Chem.* **2006**, *54* (15), 5350–5358.

(8) Wattenberg, L. W. Inhibition of carcinogenic effects of polycyclic hydrocarbons by benzyl isothiocyanate and related compounds. *J. Natl. Cancer Inst.* **1977**, *58* (2), 395–398.

(9) Zhang, Y.; Talalay, P. Anticarcinogenic activities of organic isothiocyanates: chemistry and mechanisms. *Cancer Res.* **1994**, *54* (7 Suppl.), 1976s–1981s.

(10) Conaway, C. C.; Yang, Y. M.; Chung, F. L. Isothiocyanates as cancer chemopreventive agents: their biological activities and metabolism in rodents and humans. *Curr. Drug Metab.* **2002**, *3* (3), 233–255.

(11) Hecht, S. S., *Chemoprevention by Isothiocyanates*; Humana Press: Totowa, NJ, 2004; Vol. 1, pp 21−35.

(12) Sahu, R. P.; Zhang, R.; Batra, S.; Shi, Y.; Srivastava, S. K. Benzyl isothiocyanate-mediated generation of reactive oxygen species causes cell cycle arrest and induces apoptosis via activation of MAPK in human pancreatic cancer cells. *Carcinogenesis* **2009**, *30* (10), 1744–1753.

(13) Sahu, R. P.; Srivastava, S. K. The role of STAT-3 in the induction of apoptosis in pancreatic cancer cells by benzyl isothiocyanate. *J. Natl. Cancer Inst.* **2009**, *101* (3), 176–193.

(14) Batra, S.; Sahu, R. P.; Kandala, P. K.; Srivastava, S. K. Benzyl isothiocyanate-mediated inhibition of histone deacetylase leads to NF-κB turnoff in human pancreatic carcinoma cells. *Mol. Cancer Ther.* **2010**, *9* (6), 1596–1608.

(15) Mennicke, W. H.; Gorler, K.; Krumbiegel, G.; Lorenz, D.; Rittmann, N. Studies on the metabolism and excretion of benzyl isothiocyanate in man. *Xenobiotica* **1988**, *18* (4), 441–447.

(16) Rao, J.; McClements, D. J. Formation of flavor oil microemulsions, nanoemulsions and emulsions: influence of composition and preparation method. *J. Agric. Food Chem.* **2011**, *59* (9), 5026–5035.

(17) McClements, D. J.; Rao, J. Food-grade nanoemulsions: formulation, fabrication, properties, performance, biological fate, and potential toxicity. *Crit. Rev. Food Sci. Nutr.* **2011**, *51* (4), 285–330.

(18) Anton, N.; Vandamme, T. F. Nano-emulsions and micro-emulsions: clarifications of the critical differences. *Pharm. Res.* **2011**, *28* (5), 978–985.

(19) Forgiarini, A.; Esquena, J.; González, C.; Solans, C. Formation of nano-emulsions by low-energy emulsification methods at constant temperature. *Langmuir* **2001**, *17* (7), 2076–2083.

(20) Rajpoot, P.; Pathak, K.; Bali, V. Therapeutic applications of nanoemulsion based drug delivery systems: a review of patents in last two decades. *Recent Pat. Drug Deliv. Formul.* **2011**, *5* (2), 163–172.

(21) Porter, C. J.; Charman, W. N. Lipid-based formulations for oral administration: opportunities for bioavailability enhancement and lipoprotein targeting of lipophilic drugs. *J. Recept. Signal. Transduct. Res.* **2001**, *21* (2−3), 215–257.

(22) Azeem, A.; Rizwan, M.; Ahmad, F. J.; Iqbal, Z.; Khar, R. K.; Aqil, M.; Talegaonkar, S. Nanoemulsion components screening and selection: a technical note. *AAPS PharmSciTech* **2009**, *10* (1), 69–76.

(23) Shafiq-un-Nabi, S.; Shakeel, F.; Talegaonkar, S.; Ali, J.; Baboota, S.; Ahuja, A.; Khar, R. K.; Ali, M. Formulation development and optimization using nanoemulsion technique: a technical note. *AAPS PharmSciTech* **2007**, *8* (2), article 28.

(24) Thakkar, H.; Nangesh, J.; Parmar, M.; Patel, D. Formulation and characterization of lipid-based drug delivery system of raloxifene-microemulsion and self-microemulsifying drug delivery system. *J. Pharm. Bioallied Sci.* **2011**, *3* (3), 442–448.

(25) Ganta, S.; Amiji, M. Coadministration of Paclitaxel and curcumin in nanoemulsion formulations to overcome multidrug resistance in tumor cells. *Mol. Pharmaceutics* **2009**, *6* (3), 928–939.

(26) Vyas, T. K.; Shahiwala, A.; Amiji, M. M. Improved oral bioavailability and brain transport of Saquinavir upon administration in novel nanoemulsion formulations. *Int. J. Pharm.* **2008**, *347* (1−2), 93–101.

(27) Shakeel, F.; Ramadan, W.; Ahmed, M. A. Investigation of true nanoemulsions for transdermal potential of indomethacin: characterization, rheological characteristics, and ex vivo skin permeation studies. *J. Drug Target.* **2009**, *17* (6), 435–441.

(28) Stenberg, P.; Norinder, U.; Luthman, K.; Artursson, P. Experimental and computational screening models for the prediction of intestinal drug absorption. *J. Med. Chem.* **2001**, *44* (12), 1927–1937.

(29) Youdim, K. A.; Avdeef, A.; Abbott, N. J. In vitro trans-monolayer permeability calculations: often forgotten assumptions. *Drug Discov. Today* **2003**, *8* (21), 997–1003.

(30) Liebes, L.; Conaway, C. C.; Hochster, H.; Mendoza, S.; Hecht, S. S.; Crowell, J.; Chung, F. L. High-performance liquid chromatography-based determination of total isothiocyanate levels in human plasma: application to studies with 2-phenethyl isothiocyanate. *Anal. Biochem.* **2001**, *291* (2), 279–289.

(31) Skehan, P.; Storeng, R.; Scudiero, D.; Monks, A.; McMahon, J.; Vistica, D.; Warren, J. T.; Bokesch, H.; Kenney, S.; Boyd, M. R. New colorimetric cytotoxicity assay for anticancer-drug screening. *J. Natl. Cancer Inst.* **1990**, *82* (13), 1107–1112.

(32) Waitzberg, D. L.; Torrinhas, R. S.; Jacintho, T. M. New parenteral lipid emulsions for clinical use. *JPEN* **2006**, *30* (4), 351–367.

(33) Krohn, K.; Koletzko, B. Parenteral lipid emulsions in paediatrics. *Curr. Opin. Clin. Nutr. Metab. Care* **2006**, *9* (3), 319–323.

(34) Hippalgaonkar, K.; Majumdar, S.; Kansara, V. Injectable lipid emulsions − advancements, opportunities and challenges. *AAPS PharmSciTech* **2010**, *11* (4), 1526–1540.

(35) Dahan, A.; Hoffman, A. Rationalizing the selection of oral lipid based drug delivery systems by an in vitro dynamic lipolysis model for improved oral bioavailability of poorly water soluble drugs. *J. Controlled Release* **2008**, *129* (1), 1–10.

(36) Caughey, G. E.; Mantzioris, E.; Gibson, R. A.; Cleland, L. G.; James, M. J. The effect on human tumor necrosis factor alpha and interleukin 1 beta production of diets enriched in n-3 fatty acids from vegetable oil or fish oil. *Am. J. Clin. Nutr.* **1996**, *63* (1), 116–122.

(37) Dwivedi, C.; Natarajan, K.; Matthees, D. P. Chemopreventive effects of dietary flaxseed oil on colon tumor development. *Nutr, Cancer* **2005**, *51* (1), 52–58.

(38) Rose, D. P.; Connolly, J. M. Omega-3 fatty acids as cancer chemopreventive agents. *Pharmacol. Ther.* **1999**, *83* (3), 217–244.

(39) Williams, D.; Verghese, M.; Walker, L. T.; Boateng, J.; Shackelford, L.; Chawan, C. B. Flax seed oil and flax seed meal reduce the formation of aberrant crypt foci (ACF) in azoxymethane-induced colon cancer in Fisher 344 male rats. *Food Chem. Toxicol.* **2007**, *45* (1), 153–159.

(40) Zhao, Y.; Wang, C.; Chow, A. H.; Ren, K.; Gong, T.; Zhang, Z.; Zheng, Y. Self-nanoemulsifying drug delivery system (SNEDDS) for oral delivery of Zedoary essential oil: formulation and bioavailability studies. *Int. J. Pharm.* **2010**, *383* (1−2), 170–177.

(41) Craig, D. Q. M.; Barker, S. A.; Banning, D.; Booth, S. W. An investigation into the mechanisms of self-emulsification using particle size analysis and low frequency dielectric spectroscopy. *Int. J. Pharm.* **1995**, *114* (1), 103–110.

(42) Kawakami, K.; Yoshikawa, T.; Moroto, Y.; Kanaoka, E.; Takahashi, K.; Nishihara, Y.; Masuda, K. Microemulsion formulation for enhanced absorption of poorly soluble drugs. I. Prescription design. *J. Controlled Release* **2002**, *81* (1−2), 65–74.

(43) Bali, V.; Ali, M.; Ali, J. Nanocarrier for the enhanced bioavailability of a cardiovascular agent: in vitro, pharmacodynamic, pharmacokinetic and stability assessment. *Int. J. Pharm.* **2011**, *403* (1−2), 46–56.

(44) Kumar, M.; Pathak, K.; Misra, A. Formulation and characterization of nanoemulsion-based drug delivery system of risperidone. *Drug Dev. Ind. Pharm.* **2009**, *35* (4), 387–395.

(45) Tiwari, S. B.; Amiji, M. M. Improved oral delivery of paclitaxel following administration in nanoemulsion formulations. *J. Nanosci. Nanotechnol.* **2006**, *6* (9−10), 3215–3221.

(46) Wooster, T. J.; Golding, M.; Sanguansri, P. Impact of oil type on nanoemulsion formation and Ostwald ripening stability. *Langmuir* **2008**, *24* (22), 12758–12765.

(47) Desai, A.; Vyas, T.; Amiji, M. Cytotoxicity and apoptosis enhancement in brain tumor cells upon coadministration of paclitaxel and ceramide in nanoemulsion formulations. *J. Pharm. Sci.* **2008**, *97* (7), 2745–2756.

(48) Amidon, G. L.; Lennernas, H.; Shah, V. P.; Crison, J. R. A theoretical basis for a biopharmaceutic drug classification: the correlation of in vitro drug product dissolution and in vivo bioavailability. *Pharm. Res.* **1995**, *12* (3), 413–420.

(49) Lawrence, M. J.; Rees, G. D. Microemulsion-based media as novel drug delivery systems. *Adv. Drug Deliv. Rev.* **2000**, *45* (1), 89–121.

(50) Balimane, P. V.; Han, Y. H.; Chong, S. Current industrial practices of assessing permeability and P-glycoprotein interaction. *AAPS J.* **2006**, *8* (1), E1–E13.

(51) Hubatsch, I.; Ragnarsson, E. G.; Artursson, P. Determination of drug permeability and prediction of drug absorption in Caco-2 monolayers. *Nat. Protoc.* **2007**, *2* (9), 2111–2119.

(52) Artursson, P.; Karlsson, J. Correlation between oral drug absorption in humans and apparent drug permeability coefficients in human intestinal epithelial (Caco-2) cells. *Biochem. Biophys. Res. Commun.* **1991**, *175* (3), 880–885.

(53) Artursson, P.; Palm, K.; Luthman, K. Caco-2 monolayers in experimental and theoretical predictions of drug transport. *Adv. Drug Deliv. Rev.* **2001**, *46* (1−3), 27–43.

(54) Ingels, F.; Beck, B.; Oth, M.; Augustijns, P. Effect of simulated intestinal fluid on drug permeability estimation across Caco-2 monolayers. *Int. J. Pharm.* **2004**, *274* (1−2), 221–232.

(55) Kataoka, M.; Masaoka, Y.; Sakuma, S.; Yamashita, S. Effect of food intake on the oral absorption of poorly water-soluble drugs: in vitro assessment of drug dissolution and permeation assay system. *J. Pharm. Sci.* **2006**, *95* (9), 2051–2061.

(56) Kataoka, M.; Masaoka, Y.; Yamazaki, Y.; Sakane, T.; Sezaki, H.; Yamashita, S. In vitro system to evaluate oral absorption of poorly water-soluble drugs: simultaneous analysis on dissolution and permeation of drugs. *Pharm. Res.* **2003**, *20* (10), 1674–1680.

(57) Armand, M.; Pasquier, B.; Andre, M.; Borel, P.; Senft, M.; Peyrot, J.; Salducci, J.; Portugal, H.; Jaussan, V.; Lairon, D. Digestion and absorption of 2 fat emulsions with different droplet sizes in the human digestive tract. *Am. J. Clin. Nutr.* **1999**, *70* (6), 1096–1106.

(58) Singh, H.; Ye, A.; Horne, D. Structuring food emulsions in the gastrointestinal tract to modify lipid digestion. *Prog. Lipid Res.* **2009**, *48* (2), 92–100.